Homopolyatomic Bismuth Ions, Part 2[+]

Electronic Excitations in Homopolyatomic Bismuth Cations: Spectroscopic Measurements in Molten Salts and an ab initio CI-Singles Study

Graeme Day,[a] Rainer Glaser,*[a] Noriyuki Shimomura,[b] Atsushi Takamuku,[b] and Kazuhiko Ichikawa*[b]

Abstract: The electronic excitations of the low-valence bismuth cluster cations Bi_5^{3+}, Bi_8^{2+}, and Bi_9^{5+} have been studied with experimental and theoretical techniques. The UV-visible spectra of the bismuth ions were measured in acidic chloroaluminate melts (mixture of 1-methyl-3-benzyl imidazolium chloride and $AlCl_3$). The spectra of the Bi_5^{3+} and Bi_8^{2+} ions agree fairly well with previous reports, but also revealed additional low-energy absorptions. Ab initio methods were employed to assign the experimentally observed electronic transitions of these homopolyatomic bismuth cations. Structures were optimized at the RHF, MP2, and B3LYP levels of theory by using split-valence LANL2DZ basis sets that were augmented with one and two sets of pure d functions. The computed structures agree well with the results of neutron diffraction analyses of melts. Electronically excited states of the three clusters were treated by using the CI-Singles theory. The results of these calculations were used to explain the observed UV-visible spectra. The observed electronic excitations in the UV-visible range are all found to result from transitions involving the molecular orbitals formed by 6p-atomic-orbital overlap. This leads to the necessity of using basis sets that include d-type functions, which allow for an adequate description of the bonding that results from such p-orbital overlap. Spin-orbit coupling becomes increasingly important with increasing atomic number and its consideration is necessary when describing the electronic transitions in clusters of heavy atoms. The calculations show that singlet–triplet transitions, which are made accessible by strong spin-orbit coupling, are responsible for some of the observed absorptions.

Keywords: ab initio calculations · bismuth · density functional calculations · excited states · subvalent compounds · UV-visible spectroscopy

Introduction

Besides the common Bi^{III} oxidation state, bismuth is also found in a number of low oxidation states. In fact, bismuth has become *the* classical example of an element forming a series of homopolyatomic ions. Early investigations were concerned mainly with dilute solutions of bismuth metal in $BiCl_3$ melts,[1–4] and EMF and spectroscopic studies were consistent with the presence of Bi^+, Bi_3^+, and Bi_4^{4+} ions. X-ray crystallographic studies have shown that the more complex $Bi_{24}Cl_{28}$ cluster is composed of distinct ions in the form $[(Bi_9^{5+})_2(BiCl_5^{2-})_4(Bi_2Cl_8^{2-})]$;[5, 6] these complex ions have been studied by Raman spectroscopy.[7, 8] UV-visible spectroscopy and cyclic voltammetry were used to characterize the homopolyatomic cations of the low oxidation states of bismuth, Bi_5^{3+}, Bi_8^{2+} and Bi_9^{5+}, which were isolated in molten acidic chloroaluminate melts of the $AlCl_3/NaCl$ eutectic and the 2:1 $AlCl_3/N$-(*n*-butyl)pyridinium chloride.[9–11]

The solid phases, $[Bi_5(AlCl_4)_3]$ and $[Bi_8(AlCl_4)_2]$, were isolated from the pseudo binary system Bi-($BiCl_3+AlCl_3$).[12–14] A material with composition $Bi_{10}Hf_3Cl_{18}$ also was prepared,[15] but an X-ray diffraction study of the system Bi-($2 BiCl_3+3 HfCl_4$) showed that the composition of this compound is $[(Bi_9^{5+})(Bi^+)(HfCl_6^{2-})_3]$ and not $[(Bi_5^{3+})_2(HfCl_6^{2-})_3]$. More recently, the full single-crystal analysis of $[Bi_5(AlCl_4)_3]$ that included the intramolecular structure of the Bi_5^{3+} ion was reported.[14] The Bi_5^{3+} ion was

[a] Prof. R. Glaser, G. Day
Department of Chemistry, University of Missouri-Columbia
Columbia, Missouri, 65211 (USA)
Fax: (+1)573-882-2754
E-mail: glaserr@missouri.edu

[b] Prof. K. Ichikawa, N. Shimomura, A. Takamuku
Division of Material Science
Graduate School of Environmental Earth Sciences
University of Hokkaido, Sapporo 060 (Japan)
E-mail: ichikawa@earth.ees.hokudai.ac.jp

studied with extended Hückel theory[16] and Ulvenlund et al.[17] reported RHF, MP2, and CISD results of ab initio calculations of the D_{3h}-Bi_5^{3+} structure. We have reported the results of liquid-state neutron-diffraction measurement of D_{3h} Bi_5^{3+} together with highly correlated ab initio computations that employed effective core potentials and well-polarized basis sets.[18]

We present herein the results of experimental and theoretical studies of the electronic excitations of the highly symmetric, low-valence polycations Bi_5^{3+}, Bi_8^{2+}, and Bi_9^{5+}. The UV-visible spectra of these three cations have been measured in molten solutions of 1-methyl-3-benzyl imidazolium chloride and aluminum trichloride. The structures of the ions Bi_5^{3+}, Bi_8^{2+}, and Bi_9^{5+} were also measured by neutron-diffraction analysis of the melts.[19] Geometric parameters of the isolated bismuth clusters were optimized by using Hartree–Fock theory and included electron correlation by means of perturbation and density functional theory. The optimized structures were in excellent agreement with the neutron diffraction data. The focus of the theoretical work lies with the assignment and the characterization of the electronic transitions of the three polybismuth cations by means of an ab initio single-excitation configuration-interaction approach (CI-Singles). We have used the results of such calculations to attribute the observed UV-visible absorption bands to specific electron density transitions and to assign symmetries to the electronic transitions, offering an improved treatment to that speculated by Corbett. In 1968, Corbett discussed the bonding in $[Bi_5(AlCl_4)_3]$ and predicted the correct D_{3h} structure and assigned electronic transitions based on the premise that the large 6s–6p and 6p–6d separations in bismuth[20] would allow bonding to be treated by using only the 6p orbitals.[12] In this discussion, Corbett presented, "more as an interesting observation", that such a treatment also leads to a very good correlation between the observed UV-visible spectrum and the predicted energies of allowed electric dipole transitions, derived from the calculated energy diagram and an arbitrary scaling parameter. Comparison between the excitation energies calculated by the CI-Singles approach and those predicted from the HOMO–LUMO energy gap in the cations highlights the deficiency in the free electron molecular orbital (FE-MO) approach of predicting electronic excitation energies from the eigenvalues of ab initio molecular orbitals.

Experimental Section

Syntheses: Solid $[Bi_5(AlCl_4)_3]$,[12] $[Bi_8(AlCl_4)_2]$,[12] and $[(Bi_9)_2(Bi_3Cl_{14})_2]$[21] were prepared by fusing stoichiometric mixtures of bismuth (99.9999%), distilled purified bismuth trichloride and single crystals of aluminum trichloride. 1-methyl-3-benzyl imidazolium chloride (MeBzImCl) was synthesized from equimolar amounts of 1-methyl imidazole and benzyl chloride. The product was recrystallized from acetonitrile:ethyl acetate (1:1,v/v) and its identity was confirmed by ¹H NMR spectroscopy and elemental analysis. ¹H NMR (D_2O): $\delta = 3.92$ (N-CH_3), 5.43 (N-CH_2), 7.49 (benzene), 7.53 (imidazole), 8.78 (methylene); elemental analysis calcd (%): C 63.3, H 6.2, N 13.4, Cl 17.0; found C 62.3, H 7.1, N 13.1, Cl 16.6.

Room-temperature solution of chloroaluminate: The mixture of Me-BzImCl and $AlCl_3$ was transferred into a reactor in a glove box filled with argon gas. After being sealed in the reactor glassware, the mixture was

removed from the glove box and fused at 60-80 °C to prepare the room-temperature solution of chloroaluminate.

Spectrochemical measurement: The measurement of electronic absorption spectra was carried out by using a spectroelectrochemical cell (optical path length: 1 mm) with tightcap for solutions of $[Bi_5(AlCl_4)_3]$ (ca. 0.7 mM), $[Bi_8(AlCl_4)_2]$ (ca. 0.7 mM) and $[(Bi_9)_2(Bi_3Cl_{14})_2]$ (0.2 mM) in melt of MeBzImCl/$AlCl_3$ (67 mol%) and were recorded against a reference cell that contained the melt without these polybismuth compounds.

Computational details: In the ground state, the 83 electrons of the Bi atom are distributed as KLMN 5s(2)5p(6)5d(10)6s(2)6p(3). The large number of electrons in the cations studied led us to the use of effective core potentials in place of the electrons in shells K to O ($n \sim 1-5$). The basis sets used in this investigation describe the core electrons by the Los Alamos National Laboratory 2 (LANL2) effective core potential[22, 23] and employed split-valence (double-ζ) basis sets to describe the 6s and 6p electrons. The effective core potentials were generated from Cowan's relativistic Hartree–Fock wave function of the Bi atom which incorporates Darwin and mass–velocity terms.[22] The smallest valence basis set used consists only of the 21-type 6s and 6p basis functions on each bismuth atom. When used in conjunction with the LANL2 effective core potential, this basis set is designated LANL2DZ. We also employed improved basis sets for which 1) the LANL2DZ basis functions had been augmented by a set of five pure d-type polarization functions on each bismuth atom (LANL2DZ + P) and 2) two sets of pure d-type functions were added (LANL2DZ + PP). The polarization functions used in the LANL2DZ + P basis set have Gaussian exponents of 0.185, as suggested by Huzinaga.[24] Augmentation of the LANL2DZ basis set by two sets of d-type functions with different Gaussian exponents effectively results in the optimization of the radial component of the polarization functions. The LANL2DZ + PP basis set employed two sets of d functions, one with exponent 0.229 and a second set of more diffuse d functions with exponent 0.069. Our previous work[18] has demonstrated that the Los Alamos basis sets perform very well in describing the structure and bonding of homopolyatomic bismuth when augmented by polarization functions. Replacing the inner-shell electrons by an effective core potential is not expected to cause significant error in the calculation of electronic excitations in the UV-visible range, because of the large energy gap between the O-shell ($n \sim 5$) and the valence atomic orbitals in bismuth.

The structures of the cationic clusters were completely optimized under the constraints of the stated point group symmetry (Bi_5^{3+} in D_{3h}, Bi_8^{2+} in D_{4d}, and Bi_9^{5+} in D_{3h}) at the restricted Hartree–Fock (RHF) level of theory. Higher level optimizations were performed to account for electron correlation effects by way of second-order Møller–Plesset perturbation theory (MP2),[25] including all valence electrons in the configuration space and by use of density functional theory (DFT). The well-tested and widely accepted B3LYP functional was used. The B3LYP functional combines Becke's three-parameter exchange functional (B3)[26] with the correlation functional of Lee, Yang, and Parr (LYP).[27] The stationary point structures were characterized by vibrational analysis at the MP2/LANL2DZ + PP level of theory and the absence of imaginary vibrational modes confirmed the cations to be minimum structures in their experimentally determined symmetries.

The singly excited electronic states of the three cations were studied by using single-excitation configuration interaction theory (CI-Singles).[28] The CI-Singles method treats all singly excited states as linear combinations of singly excited Slater determinants; $|\Psi\rangle = \Sigma c_i^j |\Psi_i^j\rangle$, in which $|\Psi\rangle$ is the excited state wavefunction, $|\Psi_i^j\rangle$ is a singly excited Slater determinant with an electron excited from molecular orbital i to molecular orbital j, and c_i^j are the configuration interaction coefficients. This relatively simple formalism allows for a straightforward analysis of the electron density transitions accompanying each calculated excitation from the electronic ground state.

Singlet and triplet excited states were calculated by using the three basis sets described above (LANL2DZ, LANL2DZ + P, and LANL2DZ + PP) as well as a smaller basis set, which uses a minimal basis valence description in conjunction with the LANL2 effective core potential (denoted LANL2MB). For consistency and reasons explained in the Results and Discussion section, the geometries optimized at the MP2/LANL2DZ + PP level were used for all excited state calculations.

Ab initio calculations were performed using the Gaussian 94 program[29] on a Silicon Graphics Power Challenge-L computer. Molecular orbitals and

electron density transitions were analyzed by using Schaftenaar's visualization program, MOLDEN.[30] The graphical depictions of the molecular orbitals and the electron density distributions presented in Figures 6 – 9 also can be viewed in Virtual Reality with a web browser equipped with a VRML 2.0 plugin. This material can be found at URL http://www.missouri. edu/~chemrg/vitpub/vrml/bismuth vrml.html and or under the Supporting Information associated with this article.

Results and Discussion

Structure: The electron-poor homopolyatomic bismuth cations Bi_5^{3+}, Bi_8^{2+}, and Bi_9^{5+} were successfully prepared in chloroaluminate melts. Neutron diffraction was used to resolve the structures of the polycations and their symmetries were experimentally determined to be D_{3h}, D_{4d}, and D_{3h}, respectively, in agreement with previous work.[18, 19] The structures of the three bismuth cations are shown in Figure 1 and experimental and ab initio optimized geometric param-
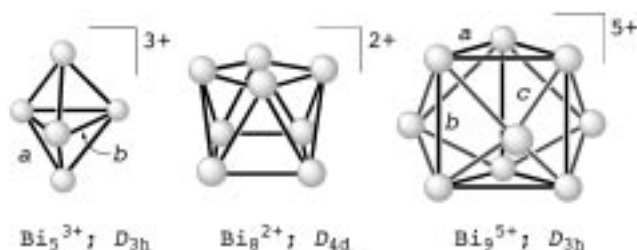

Figure 1. Symmetries of the bismuth polycations Bi_5^{3+}, Bi_8^{2+}, and Bi_9^{5+}.

eters are given in Table 1. These high-symmetry configurations were verified as energetic minima by ab initio vibrational frequency analysis at the MP2/LANL2DZ + PP level of theory. A consistent trend in the bond lengths indicates that, within a given theoretical method, basis set augmentation by a single set of polarization functions on each atom results in a shortening of the calculated bond lengths. This over-shortening of the calculated bond lengths could indicate that the set of polarization functions suggested by Huzinaga[24] are too contracted to describe the bonding in these low-valence clusters. However, the use of two sets of d-type functions, one of which is fairly diffuse, allows the polarization of the atomic

charge to relax and the bond lengths are corrected to slightly longer values. In terms of relative error (in comparison with the experimental bond lengths), the larger clusters are best described by the MP2/LANL2DZ + PP calculated geometries, while the trigonal bipyramidal trication (Bi_5^{3+}) is best described by the DFT (B3LYP/LANL2DZ + PP) optimized structure.

There is very good agreement between the bond lengths measured in the melt and those calculated in the gas phase, providing evidence that the structure and bonding in the polycations are relatively unaffected by the presence of the $AlCl_4^-$ counterions. This observation has been noted in earlier studies, where it was observed that very little change in the absorption spectrum of the Bi_8^{2+} cation was caused by changing the solvent from $NaAlCl_4/NaAl_2Cl_7$ (30:70) to $NaAlCl_4/NaCl$ (98.4:1.6).[9, 10] Furthermore, there was little noticeable change in the spectra of either Bi_5^{3+} or Bi_8^{2+} when measured in melts or in the solid that contained only $AlCl_4^-$ as a counterion.[12] The high charges of the polycations cause the HOMO levels to be highly bonding in all cases and the bismuth clusters' electronic structures should therefore only be affected by the isotropically averaged electrostatic field of the counterions and not by specific interactions.

Measured spectra: The UV-visible spectra of the homopolyatomic ions Bi_5^{3+}, Bi_8^{2+}, and Bi_9^{5+} were obtained in the chloroaluminate melt and are shown in Figures 2 – 4, respectively. The absorption spectrum of Bi_5^{3+} is characterized by twin peaks between 700 nm and 900 nm and a sharp peak at approximately 390 nm. This spectrum is in good agreement with the solution spectrum of Bjerrum et al.,[9] as well as Corbett's diffuse-reflectance and mull spectra of solid $[Bi_5(AlCl_4)_3]$.[12] The spectrum of Bi_8^{2+} displays a strong 730 nm peak and a sharp absorption at 390 nm associated with a weak shoulder near 450 nm. This spectrum agrees fairly well with the solution spectrum of Bjerrum et al.,[10] but this early work did not reveal the low-energy absorption (730 nm) that is found here. The typical spectrum of Bi_9^{5+} shows a strong peak at 450 nm and a pair of broad, weak, low-energy peaks centered at 800 nm (magnified as an insert in Figure 4).

The free electron approximation and Koopmans' theorem: The HOMO – LUMO energy gap in molecules is often used to

Table 1. Experimental and calculated bond lengths[a] in Bi_5^{3+}, Bi_8^{2+}, and Bi_9^{5+}.

Method	Bi_5^{3+}		Bi_8^{2+}	Bi_9^{5+}		
	Axial a[b]	Equatorial b[b]	All edges	Top edge a[b]	Long edge b[b]	Bi−Bi$_{cap}$ c[b]
experimental[c]	3.01	3.32	3.09 – 3.11	3.74	3.09 – 3.10	
RHF/LANL2DZ	3.0949	3.4732	3.1802	3.3635	4.1113	3.3215
RHF/LANL2DZ + P	2.9986	3.3093	3.0908	3.2231	3.8204	3.1671
RHF/LANL2DZ + PP	3.0120	3.3406	3.0983	3.2568	3.8482	3.1924
MP2/LANL2DZ	3.2049	3.4666	3.2367	3.4799	4.1341	3.4036
MP2/LANL2DZ + P	3.0561	3.2434	3.1025	3.2426	3.8012	3.1835
MP2/LANL2DZ + PP	3.0598	3.2550	3.1120	3.2659	3.8434	3.2106
B3LYP/LANL2DZ	3.1211	3.4344	3.1933	3.3797	4.1109	3.3295
B3LYP/LANL2DZ + P	3.0378	3.3053	3.1164	3.2572	3.8668	3.2013
B3LYP/LANL2DZ + PP	3.0487	3.3261	3.1216	3.2819	3.8870	3.2209

[a] All lengths in Å. [b] Symbols a, b, and c correspond to those in Figure 1. [c] Experimental data derived by neutron diffraction in the chloroaluminate melts.
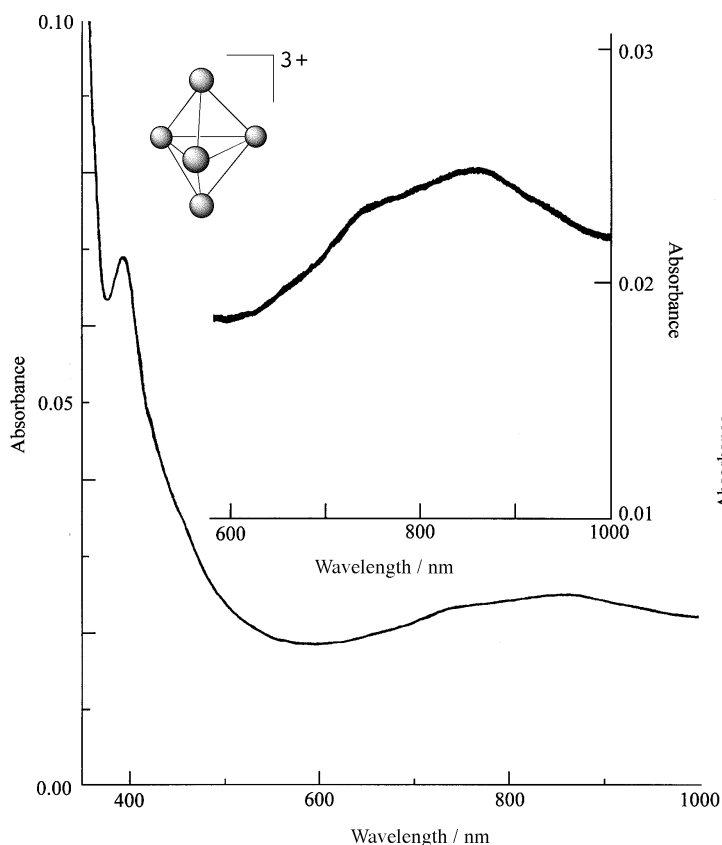
Figure 2. UV-visible absorption spectrum of Bi_5^{3+} in MeBzImCl/AlCl$_3$ (67 mol%) melt. The inset shows a magnification of the long-wavelength area.
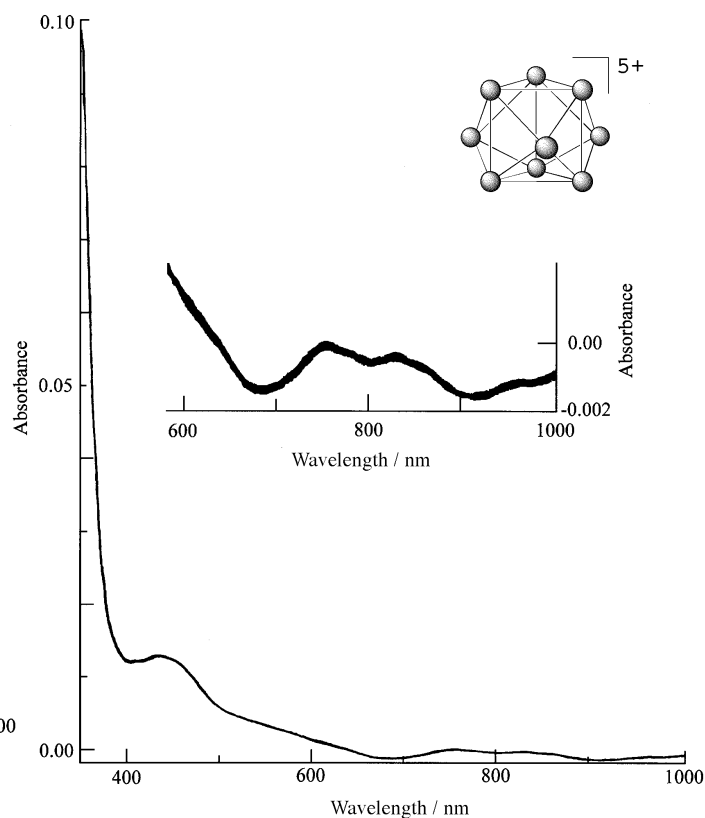

Figure 4. UV-visible absorption spectrum of Bi_9^{5+} in MeBzImCl/AlCl$_3$ (67 mol%) melt. The inset shows a magnification of the long-wavelength area.
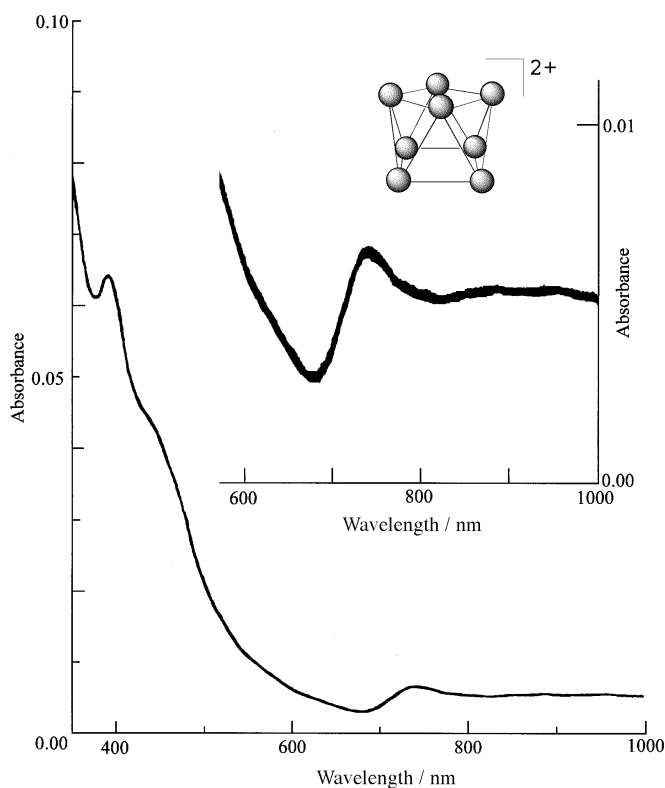

Figure 3. UV-visible absorption spectrum of Bi_8^{2+} in MeBzImCl/AlCl$_3$ (67 mol%) melt. The inset shows a magnification of the long-wavelength area.

approximate UV-visible spectra, assuming that an electron is excited from the occupied molecular orbital to the virtual orbital without affecting the orbital energies. This type of approach can be described as a free-electron molecular-orbital approximation (FE-MO) to the excitation energy. The assumptions made in this type of analysis are similar to those made by Koopmans,[31] whose theorem equates a molecule's ionization potential and electron affinity with the negative of the eigenvalue of the occupied MO and the eigenvalue of the virtual MO, respectively. There are several deficiencies with this type of analysis that we would like to highlight and provide as rationale for using the more computationally intensive CI-Singles approach to calculate the vertical excitation energies.

The well-known errors in Koopmans' treatment are the ignorance of both orbital relaxation and the change in correlation energy upon removal or addition of an electron. The CI-Singles formalism allows for both of these effects. The reorganization of the electrons upon excitation is allowed for by treating the excited wavefunction as a linear combination of singly excited states and, although Brillouin's theorem tells us that singly excited determinants will not interact directly with the reference ground state, CI-Singles calculations do not completely exclude electron correlation.[28] Furthermore, if the electronic excitation energy is taken as the difference in the eigenvalues of the occupied and virtual molecular orbitals,

we are assuming, by Koopmans' theorem, that the excitation energy is equal to the difference between the ionization potential (IP) and the electron affinity (EA). Koopmans identifies the ionization potential with the energy of the occupied orbital, but the electron affinity that is required is in fact the electron affinity of the species with an electron removed from a specific ground state orbital. For a molecule A, we would, therefore, need the electron affinity, EA(A$^+$), of the cation A$^+$ that results from ionization from a particular molecular orbital. By approximating EA(A$^+$) by the eigenvalue of the Hartree–Fock virtual orbital of the neutral molecule, Coulomb and exchange integrals are ignored and large errors are introduced that are not due to the Koopmans approximation. While still commonly used, the approximation of electronic excitation energies by HOMO–LUMO gaps goes back to the Hückel theory where electron–electron repulsion is entirely neglected. It is time that the severe deficiencies of this approach are generally recognized and that more modern methods are employed. This is not only essential to obtain more quantitative treatments, but it is absolutely essential to foster a better conceptional understanding of the energetics of absorption processes.

To illustrate the unsatisfactory excitation energies resulting from the FE-MO approach, we calculated the HOMO–LUMO energy gaps and determined the respective wavelengths of light that matches the resonance condition (Table 2). These HOMO →LUMO excitations should correspond to the longest wavelength absorption bands in the UV-visible spectra, but all calculated wavelengths are in the far UV! The considerable errors from the observed spectra highlight the need to use a more rigorous calculation to examine electronic excitations.

Table 2. HOMO–LUMO energy differences and corresponding wavelengths.

Cation	Energy[a] [kcal mol^{-1}]	Wavelength [nm]
Bi$_5^{3+}$	167.4	171
Bi$_8^{2+}$	163.4	175
Bi$_9^{5+}$	148.7	192

[a] Calculated at the MP2/LANL2DZ + PP level of theory.

Configuration interaction over all singly excited states (CI-Singles) offers an ab initio method to calculate the excited states of molecules and to facilitate the assignment of the observed absorption bands to specific electronic transitions. CI-Singles theory was used to analyze the electronic spectra of the three cations. As mentioned when discussing the agreement between ab initio and experimental structures, there is experimental evidence that the electronic structure and spectra of these bismuth polycations are unaffected by the presence of the AlCl$_4^-$ anion.[9, 10] This experimental observation is encouraging for the use of gas-phase ab initio calculations in investigations that concern the electronic transitions observed in the UV-visible energy range of such homopolyatomic clusters.

The job of assigning specific transitions to the observed absorptions was divided into two tasks. First, it was necessary

to assign symmetries to the electronic transitions observed. CI-Singles theory provides a relatively straightforward manner of determining how the orbitals transform with respect to the ground state and, hence, the molecular symmetry of the excited state. The electron density that is excited from a totally symmetric molecular orbital in the ground state results in non-zero configuration interaction coefficients in the CI-Singles output. The symmetry of the virtual orbital to which this electron density is excited reveals the electronic and, therefore, molecular symmetry of the resulting excited state. The reader should note that the corresponding density excitation from the totally symmetric orbitals of the ground state may be very small and represents only a minor part of the overall density transition involved in the excitation, but, nevertheless, it does dictate the symmetry of the excited state. This procedure is best clarified by example.

Bi$_8^{2+}$ spectral assignments: The calculated molecular orbital energy diagram for Bi$_8^{2+}$, up to the tenth virtual orbital, is shown in Figure 5. The electric dipole transition allowed
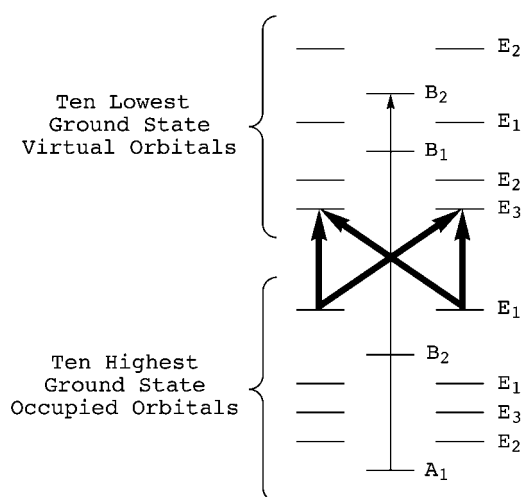
Figure 5. Orbital energy diagram of the ten highest ground state occupied orbitals and the ten lowest virtual orbitals of Bi$_8^{2+}$. The thin arrow represents the symmetry-determining orbital transition of the $e_1 \rightarrow e_3$ (B_2), while the bold arrows represent the orbital transitions that dominate the electron density transition upon excitation. (Energies are not to scale.)

excitation of calculated wavelength $\lambda \sim 406$ nm is closest in energy to the observed peak at 390 nm. The CI-Singles calculation for this excitation results in a non-zero CI coefficient ($c_{10}^{27} \sim 0.096$) that corresponds to the singly excited Slater determinant with an electron excited from the 10th (valence) molecular orbital (of A_1 symmetry) to the 27th valence molecular orbital (of B_2 symmetry). This excitation is shown by the thin arrow in Figure 5 and the orbitals involved are displayed in Figure 6. Visualization of the orbitals involved makes the symmetry transformation involved with this electronic excitation clear and allows the symmetry of the excited state to be assigned. However, the excitation of the majority of electrons that are excited from the ground state does not happen as a result of the $A_1 \rightarrow B_2$ orbital excitation. In fact, this observed absorption band results mainly from
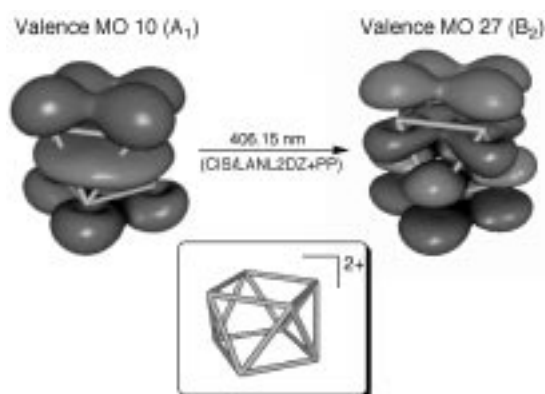
Figure 6. The $A_1 \rightarrow B_2$ orbital transition used to characterize the symmetry of the $e_1 \rightarrow e_3$ (406 nm at the CIS/LANL2DZ + PP level) electronic transition in Bi_8^{2+}.

electronic excitation between the degenerate E_1 HOMOs (valence orbitals 18 and 19) and the degenerate E_3 LUMOs (valence orbitals 25 and 26); $c_{18}^{25} \sim 0.320$, $c_{19}^{25} \sim 0.353$, $c_{18}^{26} \sim 0.353$, and $c_{19}^{26} \sim -0.320$. These molecular orbital transitions are represented by the bold arrows in Figure 5.

The above example illustrates how the symmetry of the excitations is determined and the procedure will not be outlined for each transition discussed. By noting the dominant CI coefficients resulting from the CI-Singles calculation, the nature of the transition can be assigned, as in the above example, where the transition is found to be $e_1 \rightarrow e_3$ (HOMO $\rightarrow$ LUMO). The actual transition should best be described by using all of the calculated CI-Singles coefficients; these are then used to generate figures which display the electron-density transitions that correspond to the calculated excitation energies. This procedure completes the characterization of the observed absorption bands and was used to assign the observed peaks in the three spectra.

As discussed above, the CI-Singles calculation for Bi_8^{2+} results in a singlet electric dipole allowed transition at 406 nm (at the CI-Singles/LANL2DZ + PP level); this has been characterized as $e_1 \rightarrow e_3$ ($^1B_2$). A slightly lower energy electric dipole transition (418 nm at the CI-Singles/LANL2DZ + PP level) is also calculated. This higher wavelength transition is characterized as $e_1 \rightarrow e_2$ ($^1E_1$). These calculated energies led us to assign them to the 390 nm peak and the 450 nm shoulder. As further evidence in assigning these absorptions, the oscillator strengths of these transitions were calculated as 0.0065 ($^1B_2$) and 0.0024 ($^1E_1$), respectively. Taking into account the degeneracy of the $^1E_1$ transition, the calculated oscillator strengths predict an absorbance ratio of 1.35:1 for the $^1B_2$ and $^1E_1$ bands. This is in exceptional agreement with the observed ratio of approximately 1.44:1. With good agreement of the excitation energies as well as the relative strengths of the absorptions, we are confident in making these assignments.

However, the low-energy band near 730 nm is not yet explained. No singlet electric-dipole-allowed transitions have calculated energies that are this low. CI-Singles calculations are not restricted to singlet excitations, nor should we expect the spectrum of bismuth clusters to be absent of bands that result from intersystem crossing. Because of the high atomic

number of bismuth ($Z \sim 83$), we should expect that spin-orbit coupling has significant effects on orbital energies and allowed transitions.

The effect of strong spin-orbit coupling is to make singlet-triplet excitations accessible. Both A_2 and E_3 triplet states are made accessible through spin-orbit coupling in D_{4d} point group symmetry, transforming as rotations about the z axis and the x and y axes, respectively. The lowest energy triplet $e_1 \rightarrow e_2$ ($^3E_3$) transition was calculated at 558 nm and assigned to the peak observed at 730 nm. The calculated and observed excitation energies do not agree as well as those of the singlet transitions, but the effects of spin-orbit coupling on the energies of the ground and excited states are ignored in the CI-Singles treatment, so such errors are not unexpected. The energies of magnetic dipole allowed transitions were calculated, but the agreement with the observed transition energy was found to be worse. Moreover, magnetic allowed transitions would normally result in much weaker absorptions. Therefore, the singlet $\rightarrow$ triplet transition seems likely to correspond to this absorption band. The electron-density transitions corresponding to the three excitations found for the Bi_8^{2+} cation are displayed in Figure 7.
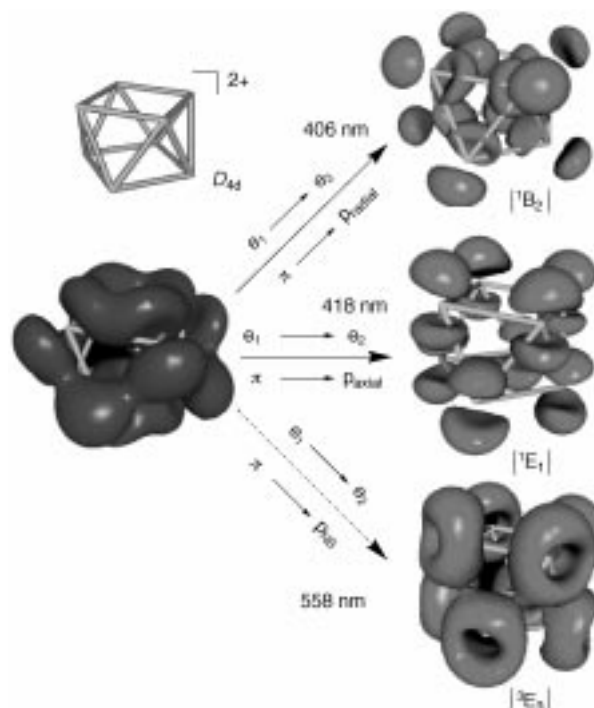

Figure 7. Calculated electron-density transitions in the UV-visible spectrum of Bi_8^{2+}. The electron density indicated on the left represents that which is lost upon excitation and that on the right corresponds to the resulting electron-density enhancement in the excited state. The wavelengths are those calculated at the CIS/LANL2DZ + PP level.

In Figure 7, the electron density depicted on the left corresponds to the electron density that is excited during the transition, while the electron density depicted on the right corresponds to the region to where the electron density is excited. A bonding skeleton of the Bi_8^{2+} polycation is given for clarity. All three of the observed absorptions correspond to the loss of electron density in the same region, which

contributes to strong π bonding around all the edges of the cation. The 390 nm transition corresponds to excitation into non-bonding p orbitals directed radially out from the center of the cation, and we describe the $e_1 \rightarrow e_3$ (B_2) density transition as $\pi \rightarrow p_{radial}$. The shoulder observed at slightly higher wavelength was found to result from a similar electronic transition, but where the electron density is excited to non-bonding p orbitals oriented in the direction of the major (S_8) axis of the cluster. Thus, we describe the $e_1 \rightarrow e_2$ ($^1E_1$) density transition as $\pi \rightarrow p_{axial}$. The triplet transition is more difficult to describe, but Figure 7 shows that it, as with the higher energy excitations, results in electron density excited out of the π-bonding region into localized, non-bonding regions that surround each bismuth atom. We, therefore, describe this density transition as $\pi \rightarrow p_{NB}$.

Bi_5^{3+} spectral assignments: The electronic spectra of the smaller Bi_5^{3+} and the larger Bi_9^{5+} polycations were analyzed and characterized in a similar fashion as for the Bi_8^{2+} cation. The 395 nm and 700 nm peaks in the Bi_5^{3+} spectrum are found to correspond to the singlet $e' \rightarrow e'$ ($^1E'$) and the triplet $e' \rightarrow e'$ ($^3A'$) transitions, respectively. The calculated wavelengths (at the CI-Singles/LANL2DZ + PP level) are slightly higher than those observed experimentally and are given in Figure 8 below, along with the corresponding density transitions. Both of these electronic transitions result in excitation out of a delocalized equatorial bonding region. The $^1E'$ transition results in the excited electron density occupying localized equatorial bonds and non-bonding density on the axial atoms, while the triplet ($^3A'$) transition at lower energy results in non-bonding electron density around each atom (see Figure 8).
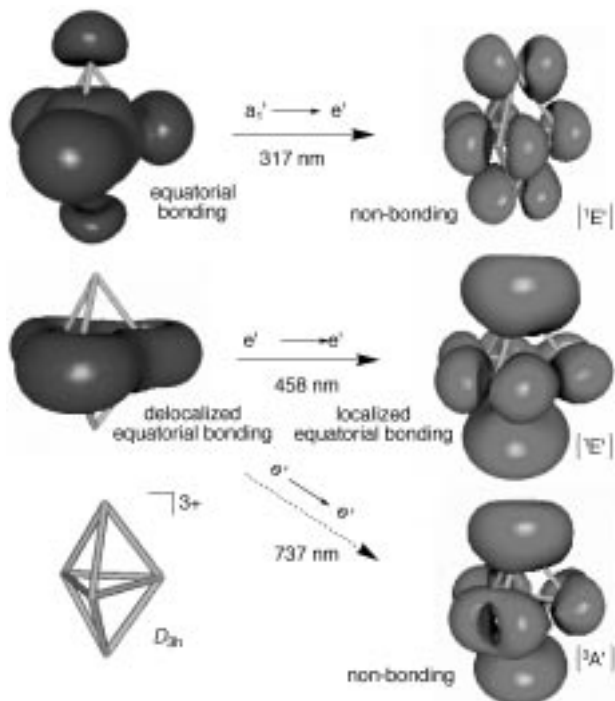

Figure 8. Calculated electron-density transitions in the UV-visible spectrum of Bi_5^{3+}. The electron density indicated on the left represents that which is lost upon excitation and that on the right corresponds to the resulting electron-density enhancement in the excited state. The wavelengths are those calculated at the CIS/LANL2DZ + PP level.

Figure 8 also shows a transition calculated at 317 nm (CI-Singles/LANL2DZ + PP), below the region measured in these studies. At these low wavelengths, the absorption of the melt is too strong to identify absorption bands that correspond to electronic transitions in the bismuth trication. However, mull spectra of $[Bi_5(AlCl_4)_3]$ crystals do reveal an absorption at 305 nm,[12] in good agreement with this calculated transition. This excitation corresponds to an $a_1' \rightarrow e'$ ($^1E'$) transition, where electron density is excited from a bonding region in which the bonding overlap is in the center of the cluster and results from radial p orbitals on the equatorial atoms and axial p orbitals on the axial atoms. Upon excitation, this electron density is excited to non-bonding p orbitals on all of the atoms. This transition is also shown in Figure 8.

We note that our assignments do not agree with those made by Corbett,[12] who employed a free electron molecular orbital (FE-MO) analysis to describe the electronic spectrum of crystalline $[Bi_5(AlCl_4)_3]$ and fitted the allowed electric dipole transitions with an arbitrary scaling parameter. The agreement between experiment and theory is fortuitously better for Corbett's FE-MO analysis than for our CI-Singles analysis. However, the CI-Singles method does not require an empirical parameter, it allows for relaxation of the electron density and is based on a more physically sound model than the FE-MO method.

Bi_9^{5+} spectral assignments: Two singlet dipole allowed transitions were calculated in the UV-visible range for the Bi_9^{5+} cation. At the CI-Singles/LANL2DZ + PP level, the calculated wavelengths are 375 nm for an $e' \rightarrow e''$ ($^1A_2''$) transition and 466 nm for a degenerate pair of $a_2'' \rightarrow e''$ ($^1E'$) transitions. Although the two excitations have calculated oscillator strengths that are almost equal ($f \sim 0.0145$ and 0.0137, respectively), the lower wavelength transition is not experimentally observed, because the absorbance of the melt masks any peaks at wavelengths below about 390 nm. However, the calculated transition at 466 nm corresponds quite well with the observed strong absorption at 450 nm. As for the smaller polybismuth cations, only singlet–triplet transitions, which are expected for clusters of heavy nuclei, have energies low enough to account for absorptions at wavelengths from 700 to 900 nm. The singlet–triplet excitation with the highest calculated wavelength corresponds to an $a_2'' \rightarrow e''$ ($^3E_2'$) transition. The wavelength is calculated to be 656 nm (CI-Singles/LANL2DZ + PP level), which is close to the observed peak at approximately 700 nm. There are no calculated transitions near the observed 900 nm absorption band, so this cannot be characterized at the moment. A more advanced calculation, taking into account the effects of spin-orbit coupling on orbital energies, is probably needed to account for this absorption. The transition densities corresponding to the three calculated excitations are displayed in Figure 9. The unobserved $e' \rightarrow e''$ ($^1A_2''$) transition corresponds to loss of radial p-orbital overlap from the capping atoms and excitation of this density to non-bonding p orbitals on the six prism atoms. The two observed transitions for which calculated excitations were found both correspond to the loss of electron density from an extended π system that bonds the capping atoms to the prism. The $a_2'' \rightarrow e''$ ($^1E'$) transition excites this
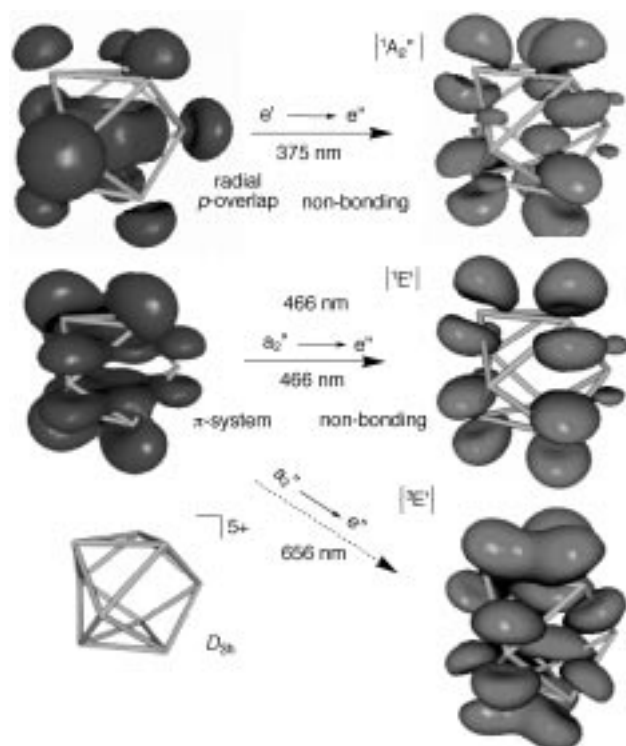
Figure 9. Calculated electron density transitions in the UV-visible spectrum of Bi_9^{5+}. The electron density indicated on the left represents that which is lost upon excitation and that on the right corresponds to the resulting electron-density enhancement in the excited state. The wavelengths are those calculated at the CIS/LANL2DZ + PP level.

Table 3. Variation of calculated transition wavelengths[a] with basis set.

Bi_5^{3+}	$a_1' \rightarrow e'$ ($^1E'$)	$e' \rightarrow e'$ ($^1E'$)	$e' \rightarrow e'$ ($^3A'$)
LANL2MB	366.2	488.8	740.2
LANL2DZ	348.0	484.9	758.0
LANL2DZ + P	318.6	460.4	736.7
LANL2DZ + PP	317.0	458.1	737.3
Observed	(305)[12]	395	700
Bi_8^{2+}	$e_1 \rightarrow e_3$ ($^1B_2$)	$e_1 \rightarrow e_2$ ($^1E_1$)	$e_1 \rightarrow e_2$ ($^3E_3$)
LANL2MB	404.0	393.1	528.1
LANL2DZ	436.4	409.2	558.5
LANL2DZ + P	400.6	415.2	550.3
LANL2DZ + PP	406.2	418.3	557.5
Observed	390	450	730
Bi_9^{5+}	$e' \rightarrow e''$ ($^1A_2''$)	$a_2'' \rightarrow e''$ ($^1E'$)	$a_2'' \rightarrow e''$ ($^3E_2'$)
LANL2MB	421.8	540.2	796.0
LANL2DZ	416.2	534.6	793.3
LANL2DZ + P	378.5	469.6	663.7
LANL2DZ + PP	375.4	465.8	655.7
Observed	not observed	450	700

[a] All wavelengths in nm.

electron density to non-bonding p orbitals on the prism atoms, while the triplet $a_2'' \rightarrow e''$ ($^3E'$) transition excites this electron density to non-bonding p orbitals on the capping atoms and π-bonding along the top and bottom edges of the prism (see Figure 9).

Basis-set dependence of excitation energies: All of the above transition energies have been quoted at the CI-Singles/LANL2DZ + PP level of theory. This is the largest basis set used in this study, but the transition energies were also calculated using smaller basis sets with one or no polarization functions. It is interesting to note how the calculated transition energies change with the basis set and the calculated energies are given in Table 3 for each transition discussed above.

Table 3 shows the importance of the choice of basis set when describing the excitation energies in such clusters. The most significant observation is the improvement of the calculated wavelengths upon augmentation of the LANL2DZ basis set by polarization functions, while the differences in calculated energies using the singly and doubly polarized basis sets is very small. The most dramatic effect is shown by the calculated excitation energies for the Bi_9^{5+} polycation. All three calculated transitions are improved significantly by increasing the basis set from the LANL2DZ to LANL2DZ + P. Although the effect is most prominent for the largest cation (Bi_9^{5+}), the effect is more important in the characterization of the transitions of the two smaller cations. The energies of the two singlet transitions observed in Bi_8^{2+} actually reverse order

upon augmentation of the double-ζ basis set with polarization functions. Should the LANL2DZ energies be used in characterizing the transitions, one could have mistakenly assigned the $e_1 \rightarrow e_3$ ($^1B_2$) transition to the observed 450 nm and the $e_1 \rightarrow e_2$ ($^1E_1$) transition to the 390 nm observed absorption. The oscillator strengths do aid in making the assignments, but the calculated energies from the LANL2DZ basis set would have made unambiguous assignments impossible. The calculated energies of the electronic transitions in the Bi_5^{3+} cluster do not change order, but the results of calculations employing either unpolarized basis set make the $a_1' \rightarrow e'$ ($^1E'$) transition seem closer in energy to the observed 395 nm absorption band than to the $e' \rightarrow e'$ ($^1E'$) transition.

The importance of including d-type polarization functions in the basis set is evident after viewing the corresponding electron density transitions. All of the observed transitions are dominated by transitions between π bonds and p orbitals, which can only be adequately described by allowing for polarization of the 6p orbitals.

Conclusion

Three homopolyatomic bismuth clusters Bi_5^{3+}, Bi_8^{2+}, and Bi_9^{5+} were prepared in chloroaluminate melts, their UV-visible spectra were measured, and their geometries were studied by neutron diffraction in the melts. Ab initio techniques were employed to assign these electronic transitions based on their transition energies and intensities, and to characterize the nature of the electronic reorganizations associated with these excitations.

The calculated geometries agree fairly well with the experimentally determined structures when a doubly polarized basis set is used; the symmetries of the cations were confirmed by vibrational frequency analysis at the MP2/

LANL2DZ + PP level of theory. We have shown that the CI-Singles formalism allows for facile interpretation of the electronic spectra. The configuration interaction approach allows for the interpretation to be made in terms of electron-density transitions, as opposed to a Koopmans' analysis, such as that suggested by Corbett,[12] which does not allow for density relaxation upon excitation of the electron. Besides a few exceptions, the excitation energies calculated with the LANL2DZ + PP basis set give good agreement with the observed UV-visible spectra. The spectra of all three cations involve singlet–triplet crossings, which is not surprising for atoms of high atomic number, when strong spin-orbit coupling allows intersystem crossings. All of the observed transitions involve either p orbitals or π bonds, which make the use of d-type polarization functions necessary for calculating accurate excitation energies.

[1] S. J. Yosim, A. J. Darnell, W. G. Gehman, S. W. Mayer, *J. Phys. Chem.* **1959**, *63*, 230.

[2] L. E. Topol, S. J. Yosim, R. A. Osteryoung, *J. Phys. Chem.* **1961**, *65*, 1511.

[3] C. R. Boston, G. P. Smith, L. C. Howick, *J. Phys. Chem.* **1963**, *67*, 1849.

[4] J. D. Corbett, F. C. Alber, R. A. Sallach, *Inorg. Chim. Acta* **1968**, *2*, 22.

[5] A. Hershaft, J. D. Corbett, *Inorg. Chem.* **1963**, *2*, 979.

[6] R. M. Friedman, J. D. Corbett, *Inorg. Chim. Acta* **1973**, 7.

[7] R. C. Burns, R. J. Gillespie, W. C. Luk, *Inorg. Chem.* **1978**, *17*, 3596.

[8] K. Ichikawa, K. Fukushi, *J. Raman Spectrosc.* **1986**, *17*, 139.

[9] N. J. Bjerrum, C. R. Boston, G. P. Smith, *Inorg. Chem.* **1967**, *6*, 1162.

[10] N. J. Bjerrum, G. P. Smith, *Inorg. Chem.* **1967**, *6*, 1968.

[11] L. Heerman, W. D'Olieslager, *J. Electrochem. Soc.* **1991**, *138*, 1372.

[12] J. D. Corbett, *Inorg. Chem.* **1968**, *7*, 198.

[13] B. Krebs, M. Hucke, C. J. Brendel, *Angew. Chem.* **1982**, *94*, 453; *Angew. Chem. Int. Ed. Engl.* **1982**, *21*, 445.

[14] B. Krebs, M. Mummert, C. J. Brendel, *J. Less-Common Metals* **1986**, *116*, 159.

[15] R. M. Friedman, J. D. Corbett, *Inorg. Chem.* **1973**, *12*, 1134.

[16] R. C. Burns, R. J. Gillespie, J. A. Barnes, J. McGlinchey, *Inorg. Chem.* **1982**, *21*, 799.

[17] S. Ulvenlund, K. Ståhl, L. Bengtsson-Kloo, *Inorg. Chem.* **1996**, *35*, 223.

[18] K. Ichikawa, T. Yamanaka, A. Takamuku, R. Glaser, *Inorg. Chem.* **1997**, *36*, 5284.

[19] The neutron diffraction structure of Bi_5^{3+} in the melt has been reported in ref. [18]. The details of the neutron diffraction structures of Bi_8^{2+} and Bi_9^{5+} in the chloroaluminate melt will be published elsewhere.

[20] J. D. Corbett, R. E. Rundle, *Inorg. Chem.* **1964**, *3*, 1408.

[21] J. Beck, C. J. Brendel, L. Bengtsson-Kloo, B. Krebs, M. Mummert, A. Stankowski, S. Ulvenlund, *Chem. Ber.* **1996**, 129, 1219.

[22] a) P. J. Hay, W. R. Wadt, *J. Chem. Phys.* **1985**, *82*, 270; b) W. R. Wadt, P. J. Hay, *J. Chem. Phys.* **1985**, *82*, 284; c) P. J. Hay, W. R. Wadt, *J. Chem. Phys.* **1985**, *82*, 299.

[23] Note that the LANL2DZ effective core potential is unchanged from the LANL1DZ effective core potential for bismuth.

[24] *Gaussian Basis Sets for Molecular Calculations* (Ed.: S. Huzinaga), Elsevier, New York, New York, **1984**, p. 23 ff.

[25] a) C. Möller, M. S. Plesset, *Phys. Rev.* **1934**, *46*, 618; b) M. Head-Gordon, J. A. Pople, M. J. Frisch, *Chem. Phys. Lett.* **1988**, *153*, 503; c) M. J. Frisch, M. Head-Gordon, J. A. Pople, *Chem. Phys. Lett.* **1990**, *166*, 275; d) M. J. Frisch, M. Head-Gordon, J. A. Pople, *Chem. Phys. Lett.* **1990**, *166*, 281.

[26] A. D. Becke, *J. Chem. Phys.* **1993**, *98*, 5648.

[27] a) C. Lee, W. Yang, R. G. Parr, *Phys. Rev. B* **1988**, *37*, 785; b) B. Miehlich, A. Savin, H. Stoll, H. Preuss, *Chem. Phys. Lett.* **1989**, *157*, 200.

[28] J. B. Foresman, M. Head-Gordon, J. A. Pople, M. J. Frisch, *J. Phys. Chem.* **1992**, *96*, 135.

[29] M. J. Frisch, G. W. Trucks, H. B. Schlegel, P. M. W. Gill, B. G. Johnson, M. A. Robb, J. R. Cheeseman, T. Keith, G. A. Petersson, J. A. Montgomery, K. Raghavachari, M. A. Al-Laham, V. G. Zakrzewski, J. V. Ortiz, J. B. Foresman, J. Cioslowski, B. B. Stefanov, A. Nanayak-kara, M. Challacombe, C. Y. Peng, P. Y. Ayala, W. Chen, M. W. Wong, J. L. Andres, E. S. Replogle, R. Gomperts, R. L. Martin, D. J. Fox, J. S. Binkley, D. J. Defrees, J. Baker, J. P. Stewart, M. Head-Gordon, C. Gonzalez, J. A. Pople, *Gaussian 94, Revision C.3*, Gaussian, Pittsburgh, PA, **1995**.

[30] *MOLDEN: A Portable Electron Density Program*, QCPE 619, G. Schaftenaar, *QCPE Bulletin*, **1992**, *12*, 3.

[31] T. Koopmans, *Physica* **1933**, *1*, 104.